Available online at www.sciencedirect.com

SciVerse ScienceDirect

Geochimica et Cosmochimica Acta 99 (2012) 71–86

Geochimica et Cosmochimica Acta

www.elsevier.com/locate/gca

High-precision and high-resolution carbonate ^{230}Th dating by MC-ICP-MS with SEM protocols

Chuan-Chou Shen [a,*], Chung-Che Wu [a], Hai Cheng [b], R. Lawrence Edwards [b], Yu-Te Hsieh [a], Sylvain Gallet [a,c], Ching-Chih Chang [a], Ting-Yong Li [a,d], Doan Dinh Lam [e], Akihiro Kano [f], Masako Hori [a,g], Christoph Spötl [h]

[a] *High-Precision Mass Spectrometry and Environment Change Laboratory (HISPEC), Department of Geosciences, National Taiwan University, Taipei 10617, Taiwan, ROC*

[b] *Department of Earth Sciences, University of Minnesota, Minneapolis, MN 55455, USA*

[c] *Géoazur, CNRS UMR6526, UNS, Parc-Valrose, 06108 Nice, France*

[d] *School of Geographical Sciences, Southwest University, Chongqing 400715, People's Republic of China*

[e] *Institute of Geology, Vietnamese Academy of Science and Technology, Hanoi, Viet Nam*

[f] *Division of Evolution of Earth Environment, Graduate School of Social and Cultural Studies, Kyushu University, Japan*

[g] *Earth Dynamic System Research Center, National Cheng Kung University, No. 1, University Road, Tainan City 701, Taiwan, ROC*

[h] *Institute of Geology and Paleontology, University of Innsbruck, Innrain 52, 6020 Innsbruck, Austria*

Received 4 February 2012; accepted in revised form 11 September 2012; Available online 26 September 2012

Abstract

To facilitate the measurement of U–Th isotopic compositions suitable for high-precision and high-resolution ^{230}Th dating of coral and speleothem carbonates, secondary electron multiplier (SEM) protocol techniques for multicollector inductively coupled plasma mass spectrometry (MC-ICP-MS) have been developed. The instrumental sensitivities are 1–2%, with a precision of ±1–2‰ (2σ) for abundance determination of 50–200 fg ^{234}U (1–4 ng ^{238}U) or ^{230}Th. This method features chemistry refinements, improvements to procedural and instrumental blanks, spectral inference reductions, and careful consideration of non-linear SEM behavior. Measurement consistency of this MC-ICP-MS combined with previous mass spectrometric results on U–Th standards and a variety of carbonates demonstrates the validity of the SEM protocol method. For fossil corals, a routine U–Th isotopic determination at permil-level precision requires only 10–50 mg of carbonate. As little as 200 mg of young coral with an age of less than 20 yr can be dated with a precision of ±0.3–0.8 yr. About 20–200 mg speleothem samples with sub-ppm-to-ppm U are required to earn a 5‰ precision on ages from 5 to 100 kyr. Requirement of small sample size, 10–100s mg carbonate, can permit high temporal resolution to date speleothems with slow growth rates, i.e., 1–10 mm/kyr. This high-precision ^{230}Th chronology is critical to accurately establish age models, date events and splice geochemical proxy time series records from multiple samples in the fields of paleoclimatology and paleoceanography. The U–Th isotopic determination techniques described here can also be applied to different environmental samples, such as waters, rocks, and sediments.

1. INTRODUCTION

Carbonates, such as marine corals and speleothems, are widely used as climatic and environmental archives (e.g., Shen, 1996; Gagan et al., 2000; Edwards et al., 2003; Fairchild et al., 2006; Grottoli and Eakin, 2007; Cheng et al., 2009; Fairchild and Treble, 2009; Lachniet, 2009; Shen et al., 2010; DeLong et al., 2012; Kanner et al., 2012). One of the most important advantages of these archives is that ^{230}Th dating techniques offer precise chronologies for proxy records over the last 600 thousand years (kyr) (e.g., Edwards et al., 1986/87; Wang et al., 2001; Edwards

* Corresponding author. Tel.: +886 2 33665878; fax: +886 2 33651917.

E-mail address: river@ntu.edu.tw (C.-C. Shen).

0016-7037/$ - see front matter © 2012 Elsevier Ltd. All rights reserved.
http://dx.doi.org/10.1016/j.gca.2012.09.018

et al., 2003; Richards and Dorale, 2003; Wang et al., 2004, 2008; Andersen et al., 2008; Cheng et al., 2009, 2012a; Stirling and Andersen, 2009; Zhao et al., 2009). Weekly-to-decadal resolved ^{230}Th-dated climate coral and speleothem records over the last glaciation have been reconstructed with precisions of ±10–100s yr (e.g., Wang et al., 2001, 2005; Cobb et al., 2003; Yuan et al., 2004; Fleitmann et al., 2007; Cheng et al., 2009; Griffiths et al., 2009; Siklósy et al., 2009; Shen et al., 2010; Jiang et al., 2012; Li et al., 2011; Sinha et al., 2011; Kanner et al., 2012).

Following the α-counting methods from the 1950s (e.g., Barnes et al., 1956; Broecker and Thurber, 1965; Ivanovich and Harmon, 1992; Bourdon et al., 2003), thermal ionization mass spectrometry (TIMS) techniques with permil-level precision have offered significant advantages in ^{230}Th dating since the 1980s (e.g., Chen et al., 1986; Edwards et al., 1986/87). In the 1990s, a number of inductively coupled plasma mass spectrometric (ICP-MS) techniques were developed to promote higher throughput and increased versatility. These include: ICP-quadrupole (Q)-MS (e.g., Shaw and Francois, 1991; Shen et al., 2006; Douville et al., 2011), ICP-sector field (SF)-MS (e.g., Shen et al., 2002), and multicollector (MC)-ICP-MS (e.g., Luo et al., 1997; Halliday et al., 1998; Goldstein and Stirling, 2003).

With an instrumental sensitivity of 1–2% for the latest generation of MC-ICP-MS in the 2000s, epsilon-level precision can be achieved with Faraday cup protocols using 20–40 pg ^{234}U (400–800 ng of ^{238}U). These capabilities have been applied to frontier topics, such as the tracing of riverine U in Arctic seawater (Andersen et al., 2007) and accurate ^{230}Th dating of 500 kyr-old carbonates with a precision of ±4–8 kyr (Cheng et al., 2012a). Despite refinements of MC-ICP-MS techniques (e.g., Goldstein and Stirling, 2003 and reference therein; Andersen et al., 2004, 2007, 2008; Hoffmann et al., 2005, 2007; Stirling et al., 2007; Ball et al., 2008; Cheng et al., 2009; Stirling and Andersen, 2009), difficulties still exist for U–Th isotopic determinations with SEM methods, particularly those associated with SEM characteristics (Richter et al., 2001, 2009; Hoffmann et al., 2005; Ball et al., 2008), spectral interferences (e.g., Pietruszka et al., 2002; Shen et al., 2002), and procedural blanks (e.g., Shen et al., 2003, 2008).

To establish high-precision and high-resolution carbonate ^{230}Th dating techniques for precise cross-correlation of proxy records and accurate determination of the timing of climatic events with precisions of ±1–10s yr or better, we developed a MC-ICP-MS technique with single-SEM protocols as follows. First, labware cleaning processes and chemistry procedures were modified from the methods proposed by Edwards (1988) to effectively reduce spectral interferences and procedural blanks. Second, the SEM behavior was carefully addressed using uranium standard solutions with different ion beam intensities, 10^2-10^6 counts per seconds (cps) and different spiking ratios, ^{235}U/^{233}U = 10–4750. Third, an 18-month measurement period of U standards was performed to evaluate reproducibility. Fourth, international and in-house U and Th standards and diverse carbonate samples were analyzed to examine precision and accuracy of this methodology. Fifth, coeval 10–100s mg coral and stalagmite subsamples with ages from <10 yr to 110 kyr were ^{230}Th-dated to evaluate the improvements in chemistry procedures and instrumentation. Finally, the developed MC-ICP-MS technique with SEM protocols was applied to natural coral and speleothem examples. A precise age model using ^{230}Th dates with errors of ±0.4–0.5 yr was built for a 35-cm living *Porites* coral head, with a hiatus at 13.5 cm from the top, collected from the western South China Sea. Another example given is that a high-resolution chronology (19 ^{230}Th dates with precision of ±10s yr) was established for a 27-mm depth interval of a Japanese stalagmite which grew at a slow rate of 5–15 mm/kyr.

2. EXPERIMENTAL

2.1. Storage and subsampling

To keep procedural blanks low, sampling and subsampling procedures were improved and contamination-free storage and workbench spaces were used. Young and old samples were double-bagged individually and isolated in different storage places. For modern and fossil corals with porous skeletons, samples were protected in individual bags to avoid cross contamination in the field. Different natural carbonates, such as coral, speleothem, sclerosponge, and tufa were stored separately (Shen et al., 2008).

Subsampling was performed on class-100 laminar flow benches in a class-10,000 subsampling room. Separated benches with independent labware were used for different samples with diverse U–Th levels. The drilled/sawed subsamples were collected in acid-cleaned plastic vials. Coral subsamples were further ultrasonicated 4–5 times prior to chemical treatment (Shen et al., 2007, 2008).

2.2. Standards and samples

Two international standards, New Brunswick Laboratories Certified Reference Material 112A (NBL-112A, also called CRM-145 or formerly NBS SRM-960), and Harwell uraninite, HU-1, were used. Ames Th standard solution, with a low ^{230}Th/^{232}Th atomic ratio of 0.603 (±0.004) × 10^{-6}, was prepared using purified thorium metal by the Standard Materials Preparation Center, Ames Laboratory, Iowa, USA (Cheng et al., 2000, 2012b). Three in-house Th standards, Th-1, Th-2, and Th-10, with ^{230}Th/^{232}Th ratios of 10^{-5}–10^{-6} were made by mixing the standards Ames Th and HU-1 (Shen et al., 2002).

One stalagmite, CC99-3, collected from Crevice Cave, Missouri, USA (37°45′N, 89°50′W; Dorale et al., 1998, 2004), one modern coral *Porites* head, from Nanwan, Kenting, Taiwan (21°57′N, 120°45′E), and one Holocene *Porites* from Stone-Cow Bridge, Kenting, Taiwan (21°57′N, 120°47′E), were prepared as in-house carbonate standard solutions, CAVE-1, CORAL-M, and CORAL-F, respectively. A flowstone sample WM1-H1 was collected from Wilder Mann Cave in the western part of the Northern Calcareous Alps of Austria (Meyer et al., 2009). Two secular equilibrium carbonates, MO-1 and Kr-3, were collected from Leana's Breath Cave, Western Australia, and Krubera Cave, Ukraine, respectively (Woodhead et al., 2006; Cheng

et al., 2012b). Stalagmite samples, YZ2 and YK2, collected from Yangzi Cave (29°47′N, 107°47′E) and Yangkou Cave (29°02′N, 107°13′E) in Chongqing, China, a stalagmite sample, Hiro-1, from Maboroshi Cave (34°50′N, 133°10′E) in Yuki, Hiroshima Prefecture, Japan, and one living 35-cm *Porites*, ST0506, at Son Tra Island, central Vietnam (16°07′N, 108°18′E; Shen et al., 2008) on June 14, 2005, were used to evaluate the validity of our developed techniques.

2.3. Chemistry

Water was purified using an ultrapure water tandem system modified with Millipore Milli-Q ACADEMIC and Milli-Q ELEMENT. Teflon bottles and beakers were cleaned in acid baths, using modified methods described in Edwards (1988). Teflon-ware was left in a 5-L glass beaker, cleaned with 50% aqua regia at room temperature for over 8 h and 90–100 °C for 8–10 h, followed by 2% boiling HCl (analytical reagent grade) for 6 h. Individual containers were then rinsed with ultrapure water and cleaned with 1% aqua regia (re-distilled grade + 0.1% HF) at 70 °C for 4–6 days. Reagents from SEASTAR or J.T. BAKER were used in chemistry.

Different benches with independent labware were used for different samples with different ages and diverse U–Th levels. After being dissolved in HNO_3 and spiked with a ^{229}Th–^{233}U–^{236}U tracer, the sample solution was added with 0.2 ml $HClO_4$ and refluxed at 90–100 °C for 6–10 h to decompose organic material. Samples were usually spiked with a $^{235}U/^{233}U$ atomic ratio of 10–30 in the mixed solution, which results in adequate precision for U concentration and isotopic composition determinations (Edwards et al., 1986/87; Cheng et al., 2000; Shen et al., 2002). Uranium and thorium were purified with chemical methods, similar to those described by Edwards et al. (1988) and Shen et al. (2003), including Fe co-precipitation and anion-exchange chromatography. After the final column separation step the separated U and Th aliquots were further treated with 0.05–0.2 ml $HClO_4$, refluxed with beaker cap closed at 90–100 °C for 5–8 h, and dried to effectively remove organic material and reduce this polyatomic interference. U and Th fractions were then dissolved in 1% HNO_3 (+0.05% HF) for instrumental analysis.

The improved chemical procedure results in low U–Th blank levels. Procedural blanks were measured regularly and six-month average values were 0.02 ± 0.01 pmol ^{238}U, 0.002 ± 0.002 pmol ^{232}Th, and 0.0003 ± 0.0003 fmol ^{230}Th. For the young coral and stalagmite samples with ages less than 500 yr and low ^{232}Th content, the procedural ^{232}Th and ^{230}Th blanks are as low as 0.0005 ± 0.0005 pmol and 0.0002 ± 0.0001 fmol, respectively, which is 2–2.5 times lower than previous values (Shen et al., 2008; Ludwig et al., 2011). The low ^{230}Th blank corresponds to an age error less than ± 0.1 yr for 0.5 g late Quaternary coral samples.

2.4. Instrumentation

2.4.1. Instrumental settings and abundance sensitivity

A high resolution MC-ICP-MS, Thermo Fisher NEPTUNE housed at the High-precision Mass Spectrometry and Environment Change Laboratory (HISPEC), National Taiwan University, was employed, equipped with eight movable Faraday cups, one fixed central cup, one MasCom secondary electron multiplier (SEM), SEV TE-Z/17, and four multiple ion counters. The initial kinetic energy spread of ions was reduced to ~5 eV with a grounded platinum guard electrode, decoupling the plasma from the load coil, in the plasma interface. A retarding potential quadruple lens (RPQ), acting as a selective filter for ions with disturbed energy or angle in front of the SEM can be tunable to improve abundance sensitivity. The MC-ICP-MS was operated at low resolution ($M/\Delta M = 400$). Radio frequency (RF) power was set at 1100–1200 W. Argon flow rates were set at 16 L/min for the plasma gas, 0.8–1.0 L/min for the auxiliary gas and 0.7–0.9 L/min for the sample gas. The detailed instrumental description is available in Wieser and Schwieters (2005).

A dry introduction system, Cetac ARIDUS, with a PFA ESI-20 or ESI-50 nebulizer was used. Sample solution uptake rate was 20–70 μL/min. Combined with an X-shape skimmer cone overall sensitivity (ion detected/atom introduced) was enhanced up to 1–2%. A ^{238}U (^{235}U) ion beam of 0.4–0.8 V ($1.8–3.6 \times 10^5$ cps) could be generated by 1-ppb U with an uptake rate of 50 μL/min. The observed UH^+/U^+ and ThH^+/Th ratios are in the range of 10^{-7} and UO^+/U^+ and ThO^+/Th^+ ratios are 1–2%. Temperatures of the spray chamber and desolvator were set at 110 °C and 160 °C, respectively. An optimal condition was given with a sweep Ar flow rate of 4–6 L/min and a N_2 gas flow rate of 5–25 mL/min.

Different sources of background noise and interference affect ICP-MS systems (e.g., Shen et al., 2002). The dark noise of the multiplier was 0.01–0.05 cps. Using the ARIDUS nebulization system, the instrumental memory blank was about 0.01–0.04‰ from previous sample with a 5–10-min clean step. For routine isotopic measurements, instrumental blanks were only about 0–0.1 cps at 234, 0–1 cps at 233 and 236, and 30–50 cps at 235. They were measured and corrected off-line (Shen et al., 2002). The whole introduction system should be cleaned or replaced when switching from Faraday cup protocols to SEM protocols. For examples, after running samples with high ^{233}U–^{236}U ion beams of 10–100s mV for hours, the background at 233 and 236 could be up to 10–20 cps for a 2.3 V-^{238}U case of determining sensitivity abundance using unspiked NBL-112A shown in Fig. 1. The polyatomic interference of 3–20 cps, from organics or complexes, was observed at 0.35 atomic mass unit (amu) lower than U–Th isotopic masses. The isobaric polyatomic background is ~0.8 cps for ^{229}Th, ^{232}Th, ^{234}U, ^{235}U and ^{236}U (Fig. 1), and less than 0.05 cps for ^{230}Th and ^{233}U. Another spectral background is related to the abundance sensitivity, which should also be corrected.

The degree of abundance sensitivity depends on vacuum conditions (Shen et al., 2002). Without the RPQ energy filter, the vacuum spectral background is mainly from ^{238}U tailing for U (e.g., Shen et al., 2002; Ball et al., 2008). ^{235}U makes a significant contribution to the baseline over the mass interval 235.5–236.5. The abundance sensitivity of ^{238}U with 2–50 V is about 2–3 ppm at $m/z = 237.04$,

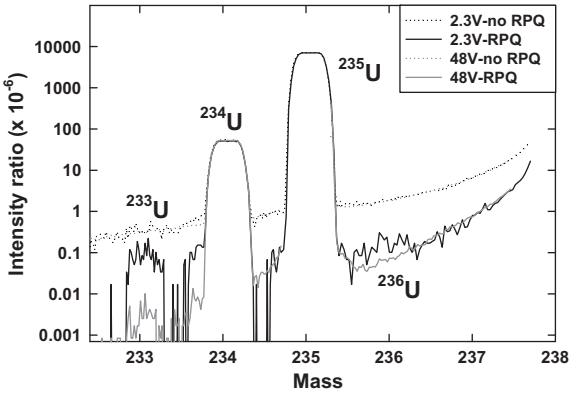

Fig. 1. The intensity ratios of counts at masses 232.4–237.7 to ^{238}U ion beam of 2.3 V (black lines) and 48 V (gray lines) with RPQ (solid lines) and without RPQ (dashed lines), for unspiked U standard NBL-112A solution. With the RPQ set to 80–85% transmission, the abundance sensitivity of ^{238}U can be improved from 1–0.1 to 0.1–0.001 ppm at 2–5 amu differences. It is notable that polyatomic interferences, 1–10 cps, exist at low-mass sides of masses 234, 235, and 236. For the 48 V-^{238}U case, the intensity of ^{235}U ion beam, 2×10^7 cps, was not measured on SEM.

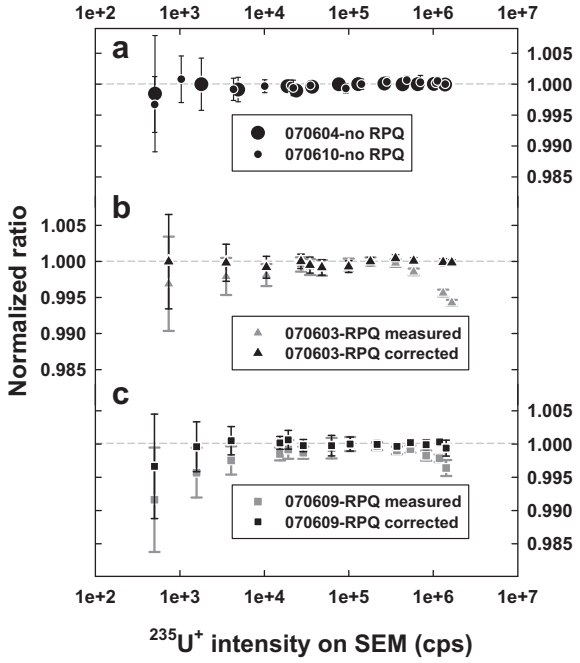

Fig. 2. Evaluation of non-linearity of the NEPTUNE SEM. Without the RPQ turned on, the normalized measured $^{235}U/^{238}U$ ratios did not vary with ^{235}U intensities from 10^2 to 10^6 with different instrumental settings on (a) June 04 (large circles) and June 10, 2007 (small circles). With the RPQ on, additional permil-level non-linearity characteristics at low- and high-intensity were variable with different instrumental settings on (b) June 03 and (c) June 09, 2007 (gray symbols). The apparent intensity biases can be fully corrected (black symbols) with empirical functions (see text).

0.4–0.7 ppm at 236.05, 0.2–0.3 ppm at 235.04, 0.2 ppm at 234.04 and 0.1 ppm at 233.04 (Fig. 1). The spectral background from ^{232}Th at low mass domain, following an exponential function, is 3–4 ppm at 231.03, 0.5–0.8 ppm at 230.03 and 0.2–0.3 ppm at 229.03. With the RPQ set to 80–85% transmission, tailing contributions were only 0.2–0.3 ppm at 1 amu difference and 0.02–0.04 ppm at 2 amu difference for ^{238}U, and 0.3–0.4 ppm and 0.04–0.06 ppm respectively for ^{232}Th.

2.4.2. Non-linearity characteristics of SEM

Precise and accurate isotopic determination requires a full understanding of SEM mass and intensity biases. Mass bias is offset from the true isotope ratio due to different SEM response related to different isotopic masses (Cheng et al., 2000). Its behavior is similar to mass discrimination and can be described by an exponential law (Cheng et al., 2000; Shen et al., 2002). There are three reported types of intensity biases. The first bias is related to multiplier dead time, which can be obtained with a precision of ±0.2 ns by measuring $^{235}U/^{233}U$ ratios in the diluted aliquots with different ^{235}U intensities of 0.3–1.5 × 10^6 cps of the same spiked uranium standard solution (Shen et al., 2002). The second intensity bias is an offset from the true ratio associated with beam intensity differences between isotopes, which can be corrected using an exponential function (Cheng et al., 2000; Shen et al., 2002). The third bias, related to the non-linearity of SEM output across the dynamic range, is observed for the previous ETP and MasCom SEMs and can be compensated with empirical algorithmic correction methods (Richter et al., 2001, 2009; Hoffmann et al., 2007). The second and third biases cannot be noticed for the latest updated MasCom SEM with an enlarged first discrete dynode (Figs. 2a and 3a).

Additional biases, different from the reported intensity bias in Cheng et al. (2000) and Shen et al. (2002), were observed in our system. They were evaluated with the RPQ on and off by comparing the measured $^{235}U/^{238}U$ ratios at different count rates. Ion beams of ^{238}U on a Faraday cup and ^{235}U on the SEM were measured simultaneously with ^{235}U intensities spanning from 500 cps to 1.4 × 10^6 cps in different diluted aliquots of uranium standard NBL-112A solution. The SEM yield drift was corrected with a precision of ±0.3‰ by running a bracketed standard aliquot with a constant ^{235}U intensity of 1–2 × 10^5 cps. The measured $^{235}U/^{238}U$ atomic ratios were normalized to the ratio with the ^{235}U intensity of 1 × 10^5 cps.

There is no difference between measured $^{235}U/^{238}U$ ratios with the RPQ off (Fig. 2a). The measured $^{235}U/^{238}U$ ratio changes distinguishably with the RPQ on (Fig. 2b and c). The intensity bias at count rates >10^5 cps, following the dead time characteristics (Hayes and Schoeller, 1977), is called apparent dead time. An additional dead time of a few nanoseconds can be applied to compensate for this bias. The exponential-function intensity bias at count rates <10^5 cps can be corrected with an empirical logarithmic algorithm, modified from Richter et al. (2001): $C_{corr} = C_{mrd}\{1 - m[\log(C_{mrd}) - \mathrm{Log}(C_N)]\}$, where C_{corr} denotes the corrected count rate, C_{mrd} the measured count rate, and C_N is the 10^5 cps base frequency for correction (Fig. 2b and c).

The additional non-linear SEM behavior is not observed for TIMS (e.g., Cheng et al., 2000). It is likely caused by the

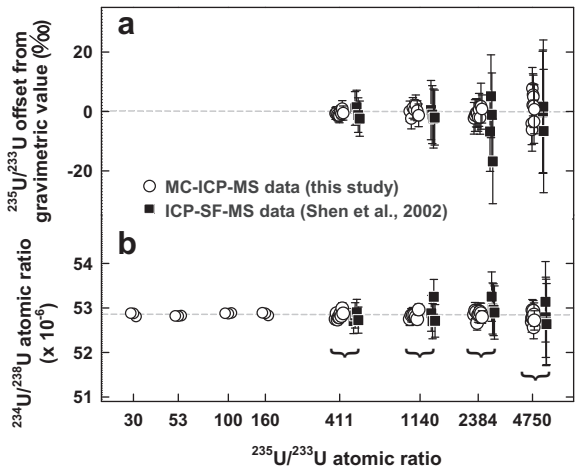

Fig. 3. Uranium isotopic measurements of under-spiked NBL-112A standard solutions. (a) No distinguishable offsets of determined $^{235}U/^{233}U$ from gravimetric values and (b) no significant difference between $^{234}U/^{238}U$ ratios with different under-spiking ratios of $^{235}U/^{233}U = 411$–4750 and 30–4750, respectively. This demonstrates the validity of the double-spike techniques and SEM non-linearity correction methods. Precision offered by the developed MC-ICP-MS techniques is better than the previous ICP-SF-MS methods with no energy filter, especially for under-spiked standard solution (solid symbols, Shen et al., 2002).

slightly defocused ions with a wide kinetic energy spread of ~5 eV in the ICP source, 10 times broader than the TIMS thermal ion source, passing through the RPQ lens to the SEM, which is installed behind the focal plane.

During the daily measurements with the same settings for the inlet system, source lenses, zoom optics, and RPQ, the rate-effect parameter, m, did not change. When the instrumental settings were re-tuned, m was observed to vary slightly. The variation of the parameter was from +0.001 to −0.002 over the course of 27 months during January 2008 to March 2010. To evaluate the validity of SEM non-linearity correction methods, U isotopic compositions of aliquots of standard NBL-112a, spiked with various $^{235}U/^{233}U$ ratios of 10–4750, and the in-house standard CAVE-1, over-spiked with a $^{235}U/^{233}U$ ratio of 5.6, were determined.

2.4.3. Data acquisition protocol and data processing

With the RPQ on, the tailing background at 236.05 amu over the ^{236}U signal ratio is 0.03–0.3‰, insignificant for U isotopic measurements with spiking ratios of $^{235}U/^{233}U$ of 10–100. The significant ^{236}U tailing background correction of >0.9‰ is necessary for isotopic determination of sample uranium with an under-spiked $^{235}U/^{233}U$ ratio >300. The spectral background at 236.44 amu was, therefore, measured to correct for the tailing background at 236.05 amu with an empirical ratio of 0.43. A scan cycle of 2.5–2.6 s, including idle time, was used to measure beam intensities of ^{233}U (0.40 s), ^{234}U (1.00 s), ^{235}U (0.26 s), ^{236}U (0.40 s) and at 236.44 amu (0.26 s). For the under-spiked sample U, integration time of ^{233}U and ^{236}U was increased.

For Th isotopic measurements, the background signals at half masses were not measured for samples with $^{230}Th/^{232}Th$ atomic ratios of $>10^{-3}$; however, the ^{232}Th tailing background was still corrected based on the determined abundance sensitivity. To measure ^{230}Th content with a precision of 1–2‰ for samples such as igneous rocks, terrestrial and marine sediments, and surface seawater that have $^{230}Th/^{232}Th$ atomic ratios $<10^{-4}$, the signal at 230.53 amu was monitored to correct for ^{232}Th tailing background with an empirical relationship. The variations of tailing characteristics result in a trivial uncertainty of <0.2‰ on Th isotopic measurements. A scan cycle of 2–4 s, including idle time, was used to measure beam intensities of ^{229}Th (0.26–1.0 s), ^{230}Th (1.0–2.0 s), and ^{232}Th (0.26 s), and at 230.53 amu (0–0.26 s).

Routine sequencing of sample U–Th measurements followed the method described in Shen et al. (2002). Th fraction was first measured 10–15 min (100–400 cycles) and then the counterpart U fraction 15–20 min (300–500 cycles). Between measurements, introduction system was cleaned with 1% HNO_3 (+0.05% HF) 4 min and instrumental blanks were measured 2 min. The total U–Th instrumental time was 30–45 min for each sample. Sample ^{232}Th and ^{235}U intensities were adjusted to $<1.2 \times 10^6$ cps. For samples with low $^{230}Th/^{232}Th$ ratios, 10^{-5}–10^{-6}, beam intensities of ^{229}Th and ^{230}Th of an additional concentrated Th solution were measured to obtain high-precision $^{230}Th/^{229}Th$ ratio and [^{230}Th]. To correct for mass discrimination and mass bias, measured U–Th isotope ratios were normalized to $^{236}U/^{233}U$ value using an exponential law (Shen et al., 2002). Before and after all sample measurements each day, spiked NBL-112A aliquots with a ^{235}U intensity of $1.0–1.5 \times 10^6$ cps were analyzed. The values of apparent dead time and rate-effect parameter were obtained by correcting the measured $^{235}U/^{233}U$ and $^{234}U/^{235}U$ ratios to the values earned with our Faraday cup protocols, developed by Cheng et al. (2012b). A dynamic jumping mode with three steps at 234.5, 236.0, and 237.0 amu, was used for U isotopic measurements. The two steps with 234.5 and 237.0 amu were measured on SEM with the RPQ off to obtain tailing backgrounds. The step at 236.0 amu was used to simultaneously measure ion beam intensities of ^{233}U, ^{234}U, ^{235}U, and ^{236}U with 10^{11} Ω resistors, and ^{238}U with a 10^{10} Ω resistor. The measured NBL-112A $\delta^{234}U$ is −38.6‰ equivalent to −37.0‰ using the previous ^{234}U half-live value (Cheng et al., 2000). For Th isotopic measurements, Th fraction was admixed ^{233}U–^{236}U spike, used to correct for mass discrimination. The ion beams of ^{229}Th, ^{230}Th, ^{232}Th, ^{233}U, and ^{236}U, were determined in static mode. Detailed methodology is described in Cheng et al. (2012b).

The SEM biases, spectral background, instrumental blanks, mass discrimination, and errors associated with quantifying the isotopic composition in the spike solution were calculated in an off-line data reduction process, modified from Shen et al. (2002). The validity of using $^{236}U/^{233}U$ measurement to correct for the following Th mass discrimination was verified using different in-house Th standards. Decay constants used are 9.1705×10^{-6} yr^{-1} for ^{230}Th and 2.8221×10^{-6} yr^{-1} for ^{234}U (Cheng et al., 2009, 2012b), and 1.55125×10^{-10} yr^{-1} for ^{238}U (Jaffey et al., 1971). Uncertainties in the U–Th isotopic data and ^{230}Th dates given in this paper are calculated at the 2σ level

or two standard deviations of the mean ($2\sigma_m$) unless otherwise noted.

2.4.4. Determination of ^{238}U content

The sample ^{238}U concentration ([^{238}U]) is calculated from [^{235}U] measurement and a known $^{238}U/^{235}U$ atomic ratio, determined with cup-protocol techniques. If $^{238}U/^{235}U$ is not available, the precision and accuracy of U-series chronologies could be compromised by $^{238}U/^{235}U$ variability (Stirling et al., 2007; Weyer et al., 2008; Brennecka et al., 2010). A range of 1.3‰ was reported in natural samples, such as basalts, granites, seawater, river water, corals, speleothems, sediments, and ferromanganese crusts (e.g., Stirling et al., 2007; Weyer et al., 2008). Based on a new isotopic standard, IRMM-074/10 with a $^{238}U/^{235}U$ ratio of 1.000259 (Richter et al., 2009), the mean $^{238}U/^{235}U$ value is 137.818 for terrestrial materials (Hiess et al., 2012). This value with an uncertainty of ±0.65‰ (Stirling et al., 2007; Andersen et al., 2008; Weyer et al., 2008; Hiess et al., 2012) is suggested to be applied for [^{238}U] calculation if the $^{238}U/^{235}U$ ratio is unknown.

For samples with trivial $^{238}U/^{235}U$ variation, a small uncertainty of <±1‰ can be applied. $^{238}U/^{235}U$ ratios of modern and fossil corals and of seawater samples, for example, are consistent within epsilon-level errors (Stirling et al., 2007; Andersen et al., 2008; Weyer et al., 2008). For this case, marine carbonate [^{238}U] can be calculated from [^{235}U]. Speleothem $^{238}U/^{235}U$ ratios vary over 1‰ between caves worldwide, but only less than ±0.2‰ within a single cave (Cheng et al., 2012b). A cave-specific $^{238}U/^{235}U$ ratio, determined by cup measurement, with an uncertainty of ±0.2‰, can be applied for [^{238}U] calculation.

3. RESULTS AND DISCUSSION

3.1. Isotopic determination of under-spiked NBL-112A

Determinations of $^{235}U/^{233}U$ and $^{234}U/^{238}U$ of different under-spiked NBL-112A aliquots are plotted in Fig. 3. For both $^{235}U/^{233}U$ and $^{234}U/^{238}U$ ratios, the between-run precisions are similar to, or better than within-run values. This observation indicates that all uncertainties are accounted for, and that the internal error is an accurate measure of the true uncertainty.

No distinguishable offsets of measured $^{235}U/^{233}U$ ratios from gravimetric values for $^{235}U/^{233}U = 411–4750$ show that non-linear SEM characteristics are fully described. The determined $^{234}U/^{238}U$ atomic ratios of different aliquots with diverse under-spiking ratios of $^{235}U/^{233}U = 30–4750$ are consistent within analytical error (Fig. 3b). The results clearly reflect the accuracy of our developed techniques. In addition, the consistency between measured and gravimetric $^{235}U/^{233}U$ values for different spiked aliquots indicates that our technique can be used to accurately analyze Th for samples with diverse $^{230}Th/^{232}Th$ ratios.

3.2. Precision and long-term reproducibility

Long-term performance was evaluated by running different diluted aliquots of a spiked NBL-112A solution over a 19-month period, from January 2007 to July 2008 (Fig. 4). Within-run precision is as good as ±0.3‰ for $^{235}U/^{233}U$ and ±0.7‰ for $^{234}U/^{235}U$. $^{234}U/^{238}U$ ratios were calculated using our measured $^{238}U/^{235}U$ ratio of 137.834 ± 0.021 given in Richter et al. (2010). After error propagation, internal precision ranges from ±0.4–1.7‰ on $^{235}U/^{233}U$ and ±0.8–2.7‰ on $^{234}U/^{238}U$ by running different ^{235}U intensities of 0.1–1.7 × 10^6 cps with various sample sizes of 0.2–8 ng of U (Fig. 4). No significant difference in isotopic determinations between different intensities for both $^{235}U/^{233}U$ and $^{234}U/^{238}U$ further verifies that the additional SEM biases with RPQ turned on have been corrected effectively. The long-term measured $^{234}U/^{238}U$ atomic ratio of 52.88 ± 0.09 × 10^{-6} is consistent with values with the Faraday cup protocol and on ICP-SF-MS (Shen et al., 2002).

The duplicated isotopic measurements of NBL-112A show that external precision agrees with internal precision (Fig. 5). It also suggests that the reproducibility of the U isotopic measurements mainly follows counting statistics and uncertainty sources during the instrumental analysis. With known $^{238}U/^{235}U$ ratios, samples of 200 fg of ^{234}U (4 ng of ^{238}U) can give precisions of 1‰ for $^{234}U/^{238}U$ ratios and 0.5‰ for [^{238}U]. If $^{238}U/^{235}U$ is not available, the natural uncertainty of ±0.65‰ (Stirling et al., 2007; Andersen et al., 2008; Weyer et al., 2008; Hiess et al., 2012) should be propagated in the calculations of $^{234}U/^{238}U$ ratio and [^{238}U].

3.3. Uranium in HU-1 and CAVE-1

Determined $\delta^{234}U$ values of HU-1 and CAVE-1 are plotted in Fig. 6. Similar to NBL-112A, HU-1 samples with

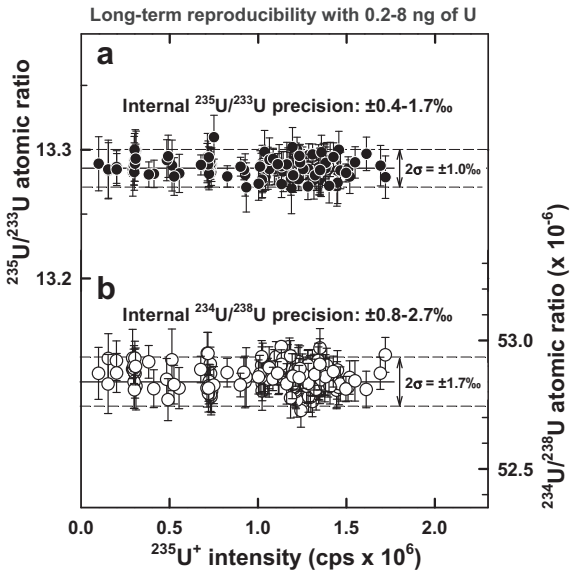

Fig. 4. Long-term reproducibility of (a) $^{235}U/^{233}U$ and (b) $^{234}U/^{238}U$ ratios on aliquots with different ^{235}U ion beam intensities of 0.2–1.7 × 10^6 cps for a spiked U standard NBL-112A solution over a course of 19 months (January 2007–July 2008). Dashed lines denote the overall external 2-sigma ranges.

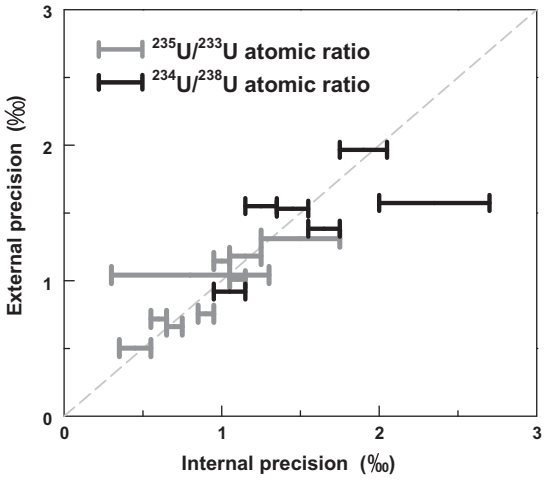

Fig. 5. The relationship between the external precision and internal precision for $^{235}U/^{233}U$ and $^{234}U/^{238}U$ ratios in Fig. 4. Data generally lie on a 1:1 line, indicating that uncertainty sources have been fully considered and the internal error is an appropriate measure of the true uncertainty.

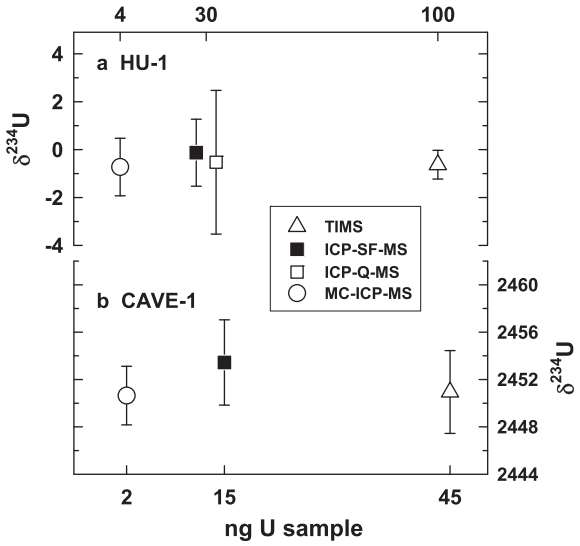

Fig. 6. $\delta^{234}U$ determinations of (a) HU-1 and (b) CAVE-1 by TIMS (triangles), ICP-SF-MS (solid squares) (Shen et al., 2002), ICP-Q-MS (hollow squares) (Shen et al., 2006), and MC-ICP-MS (circles) (this study).

4 ng ^{238}U (200 fg ^{234}U) can give an internal precision of 1‰. With the 3.6-times ^{234}U abundance in CAVE-1, only 2 ng ^{238}U (400 fg ^{234}U) is required for $^{234}U/^{238}U$ determinations with an internal precision of ±0.7‰. $\delta^{234}U$ determinations of the two standards measured by this SEM protocol are not significantly different from two previous ICP-MS methods (Shen et al., 2002, 2006), and TIMS technique (Fig. 6). For example, the $\delta^{234}U$ results, calculated with a $^{238}U/^{235}U$ ratio of 137.76 determined by Faraday cup protocols, for HU-1 are -0.7 ± 1.2 by MC-ICP-MS, -0.1 ± 1.4 by ICP-SF-MS and -0.6 ± 0.6 by TIMS.

3.4. Thorium in-house standard measurements

Concentrations of ^{232}Th and ^{230}Th, and $^{230}Th/^{232}Th$ ratios for three Th standards were measured. Th-1, Th-2 and Th-10 all have low $^{230}Th/^{232}Th$ ratios, at $2.222 \pm 0.007 \times 10^{-6}$, $3.651 \pm 0.010 \times 10^{-6}$, and $16.13 \pm 0.04 \times 10^{-6}$, respectively. The concentration and isotopic data from MC-ICP-MS, ICP-SF-MS, and TIMS measurements are all consistent with gravimetric values within error (Fig. 7). This indicates the MC-ICP-MS technique can be accurately applied to determinations of isotopic composition and concentration for low $^{230}Th/^{232}Th$ samples. Only 50 fg ^{230}Th are needed to obtain a precision of 2–5‰ for both [^{230}Th] and $^{230}Th/^{232}Th$ (Fig. 7b and c). On ICP-SF-MS, errors from tail corrections and counting statistics are significant for $^{230}Th/^{232}Th$ $<6 \times 10^{-6}$, such as Th-1 and Th-2 (Fig. 7b and c; Shen et al., 2002). On MC-ICP-MS with energy filtering, the precision is dominated by counting statistics, even with $^{230}Th/^{232}Th$ ratios as low as 2×10^{-6}.

3.5. ^{230}Th-^{234}U-^{238}U of old carbonate samples

Results from replicate analyses of six subsamples of flowstone WM1-H1 (40–98 mg with 2–3 ppm ^{238}U), are given in Table A1 and Fig. 8. Replicate measurements of $^{234}U/^{238}U$ and $^{230}Th/^{238}U$ values are consistent within er-

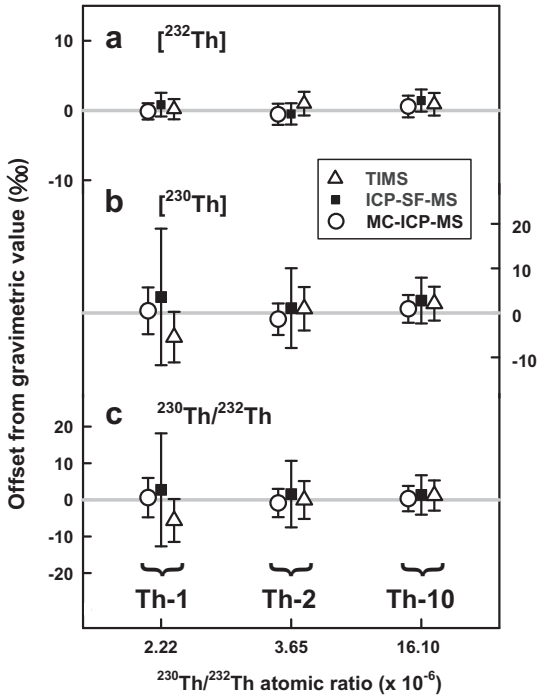

Fig. 7. Measurements of (a) [^{232}Th], (b) [^{230}Th], and (c) $^{230}Th/^{232}Th$ ratio for three Th standards with low $^{230}Th/^{232}Th$ atomic ratios of 2–16 $\times 10^{-6}$ (open circles). The data for three Th standards from measurements of TIMS (triangles), ICP-SF-MS (squares) (Shen et al., 2002), and MC-ICP-MS (circles) (this study) are all consistent within error. The observation of no significant offsets of measured data from gravimetric values demonstrates the accuracy of this methodology.

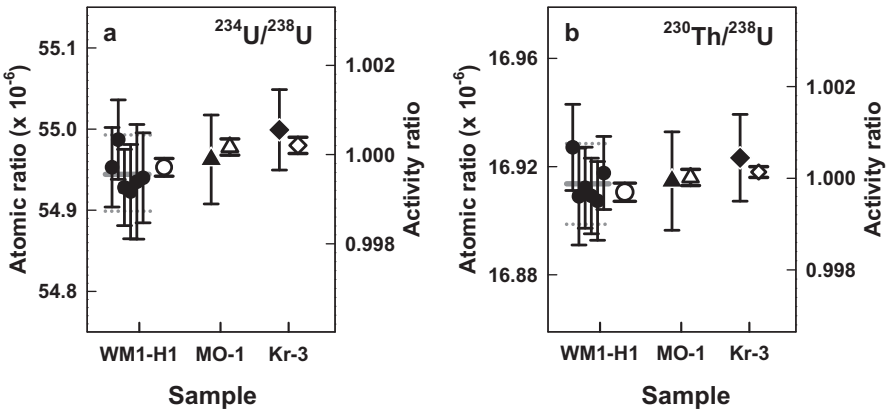

Fig. 8. Measurements of (a) $^{234}U/^{238}U$ and (b) $^{230}Th/^{238}U$ ratios for one old speleothem, WM1-H1 (solid circles), and two secular-equilibrium samples, MO-1 (solid triangle) and Kr-3 (solid diamond). For WM1-H1 measurements, the external uncertainty (gray lines) is comparable with the internal error. The $^{234}U/^{238}U$ and $^{230}Th/^{238}U$ of WM1-H1, Kr-3 and MO-1, from measurements of 1‰-precision SEM protocol and 0.2‰-precision Faraday cup methods (hollow symbols), are all consistent within error.

ror. The external uncertainties of $\pm 0.047 \times 10^{-6}$ and $\pm 0.015 \times 10^{-6}$ for $^{234}U/^{238}U$ and $^{230}Th/^{238}U$ atomic ratios are comparable to the internal uncertainties of ± 0.047–0.071×10^{-6} and ± 0.014–0.018×10^{-6}, respectively (Fig. 8). The weight-averaged activity ratios of $^{234}U/^{238}U$, 0.9996 ± 0.0004, and $^{230}Th/^{238}U$, 0.9999 ± 0.0004, are consistent with cup-protocol values, 0.9997 ± 0.0002 and 0.9997 ± 0.0002, respectively (Fig. 8). This correspondence demonstrates the overall accuracy of the chemical and instrumental techniques described here. For the two secular equilibrium carbonates, MO-1 (400 mg with 0.94 ppm ^{238}U) and Kr-3 (420 mg with 2.2 ppm ^{238}U), the measured activity ratios of $^{234}U/^{238}U$ and $^{230}Th/^{238}U$ with 0.9–1.0‰ precision match cup-protocol values (Fig. 8).

3.6. ^{230}Th dating on coral and speleothem examples

^{230}Th dates of coral and speleothem subsamples measured by MC-ICP-MS and ICP-SF-MS (Shen et al., 2002) are given in Tables A2 and A3 and plotted in Fig. 9. Only 200–400 mg of modern and fossil coral subsamples are needed to provide age precision of ±0.3 yr for an 8.8-yr-old modern coral and ±17–19 yr for a 6.9-kyr fossil coral by MC-ICP-MS (Fig. 9a), superior to precisions of ±0.6 yr and ±24–25 yr measured using ICP-SF-MS on 700–1500 mg-sized samples.

To date speleothems with [U] of 4–16 ppm and ^{232}Th levels of 2000–6000 ppt, 2-sigma age errors are ±29, ±86, ±252, and ±378 yr for samples with ages to 8.6, 23.6, 58.0, and 111 kyr, respectively, using MC-ICP-MS with only 30–120 mg carbonate consumed. The dates agree with those determined with ICP-SF-MS using 150–300 mg carbonate (Fig. 9b). The two data sets are all consistent within error and provide further evidence that high-precision U–Th isotopic measurements can be achieved with MC-ICP-MS using small samples.

3.7. High-precision and high-resolution age models

U–Th isotopic compositions of sixteen subsamples from four layers of a living *Porites* coral head, ST0506, were analyzed with MC-ICP-MS and ICP-SF-MS (Shen et al., 2002) (Table A4). The ^{230}Th dates were corrected using the site-specific initial $^{230}Th/^{232}Th$ ratio of $3.20 \pm 0.32 \times 10^{-6}$ (Shen et al., 2008). For these layers with ages <20 yr, only 170–360 mg carbonate was required to achieve a dating precision of ±0.8 yr by MC-ICP-MS techniques. In contrast, a sample size of 490–930 mg is necessary to achieve the same precision with ICP-SF-MS methods. Above the hiatus, the

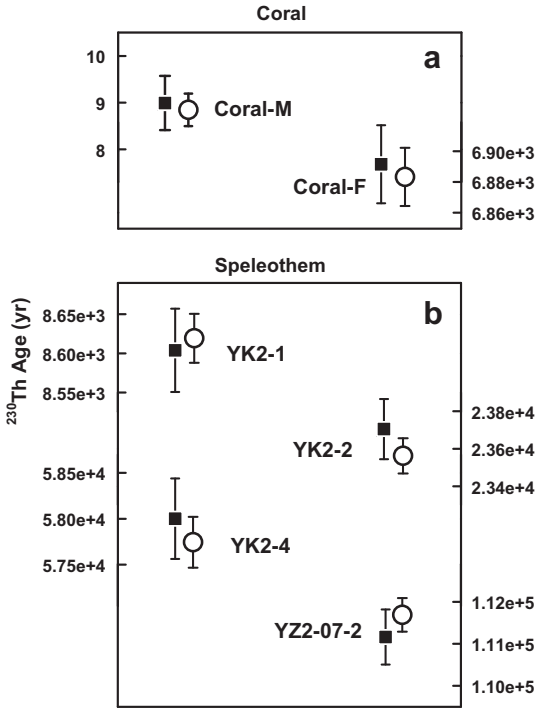

Fig. 9. Comparison of ^{230}Th ages determined on ICP-SF-MS (squares) (Shen et al., 2002), and MC-ICP-MS (circles) (this study) for (a) a modern, Coral-M, and a Holocene, Coral-F, coral *Porites*, and (b) four speleothem subsamples, YK2-1, YK2-2, YK2-4, and YZ2-07-2, with ages from 9–1.1×10^5 yr. There is no significant difference between data by the two techniques.

two mean ^{230}Th dates of AD 1998.21 ± 0.45 and AD 1996.15 ± 0.52 are consistent with dates of AD 1998.3–1998.6 and AD 1996.3–1996.6, respectively, estimated with density-band counting and geochemical proxy records (Fig. 10). Below the hiatus, the two mean ^{230}Th dates of AD 1990.45 ± 0.54 and AD 1987.59 ± 0.43 and the coral Sr/Ca record constrain the occurrence of the discontinuity to sometime after the summer of 1991 and likely the last 2–3 months at most, probably in the summer to fall of 1991.

Nineteen subsamples, 1 mm in width and 30–60 mg in weight, from a short depth interval (54–81 mm) of stalagmite Hiro-1 were drilled for high spatial resolution ^{230}Th dating (Table 1 of Shen et al., 2010). An average 2-sigma precision of ±70 yr (or 0.5%) was earned on ages from 7.88 to 15.81 kyr for the subsamples with [^{238}U] of 0.24–0.78 ppm (Fig. 11). Duplicate ^{230}Th dates for coeval subsamples at depths of 60.8, 75.0, and 81.0 mm, and all ages in stratigraphic order show the robust methodology (Fig. 11). With this high-resolution ^{230}Th dating the time spans for the two hiatuses at depths of 55.0 mm and 65.4 mm are precisely determined. The hiatuses would be difficult to be detected if wide subsampling width were required. A reliable age model can be established for this depth window with slow growth rates of 5–15 mm/kyr using the techniques described here.

3.8. Advantages and disadvantages of SEM protocol techniques

Compared to the ionization-transmission efficiencies of 0.2–2‰ on TIMS (e.g., Cheng et al., 2000) and 1–2‰ on ICP-SF-MS (Shen et al., 2002), the developed MC-ICP-MS method offers a higher efficiency of 1–2% and allows for smaller sample sizes. Coupled with the improved abundance sensitivity using the RPQ, the precision offered by the SEM protocol MC-ICP-MS technique is better than the previous ICP-SF-MS methods with no energy filter, especially for under-spiked samples (Fig. 3) with low ^{230}Th/^{232}Th atomic ratios, i.e., $<10^{-5}$ (Fig. 7). Only 1–4 ng U can offer a 2-sigma precision of ±1–2‰ for ^{234}U/^{238}U ratios. For high-precision late Quaternary carbonate ^{230}Th dating, however, 10–100s ng U is required due to relatively low ^{230}Th abundance.

For 2–3 ppm-U Holocene and Quaternary corals a routine U–Th isotopic determination at permil-level precision requires 50 mg of carbonate. Age errors <0.5–1% are possible for subsamples that are only 1–20 mg in size. A decade-century-old modern coral can be ^{230}Th-dated with precisions better than 1 yr (Fig. 10) with (1) low [^{232}Th] of 10s of ppt or (2) relatively high [^{232}Th] of 100–1000s of ppt and an initial ^{230}Th/^{232}Th variation of only 10–20%. This high-precision ^{230}Th dating can be applied to living corals with banding discontinuities, equatorial-zone corals with intrinsically small seasonal geochemical cycles and obscure density banding, and dead coral heads and fossils without absolute ages (Shen et al., 2008). The coral-inferred climatic anomalies and environmental events at the same site or different regimes can then be well-dated, spliced, coupled and/or compared, providing accurate data for retrospective understanding of global change (e.g., Cobb et al., 2003; Shen et al., 2005; DeLong et al., 2012). In addition, high-precision ^{230}Th dating in corals can provide a chronological tool to identify past abrupt events, such as earthquakes in subduction-zone settings (e.g., Taylor et al., 1990; Sieh

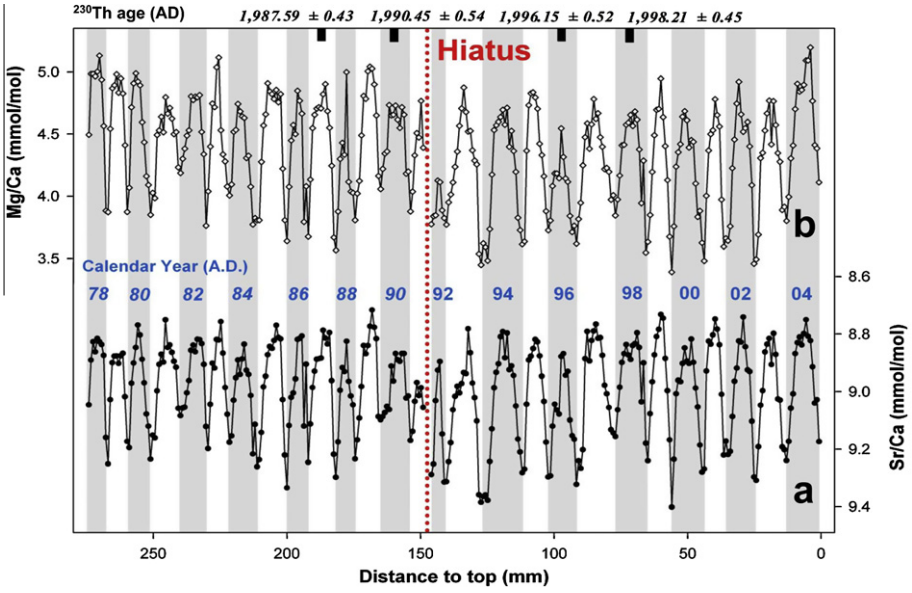

Fig. 10. ^{230}Th dates with precisions of ±0.4–0.5 yr of four layers, two above and two below a hiatus (red dotted line) at 13.5 cm from the top of a modern coral head, ST0506, collected from Son Tra Island, central Vietnam. An age model is built using the ^{230}Th dates, coupled with (a) Sr/Ca and (b) Mg/Ca records and density banding (gray-white vertical bars). The discontinuity is suggested to last 2–3 months at most in summer-fall of 1991.

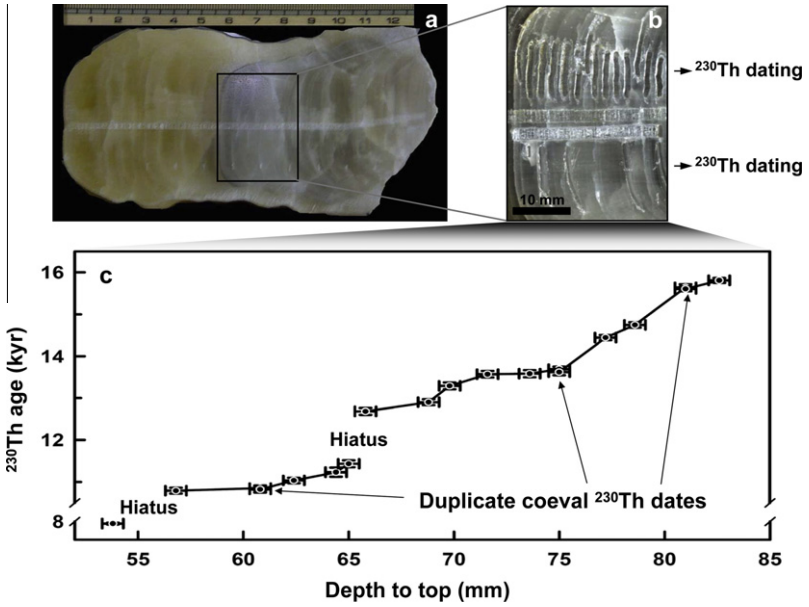

Fig. 11. (a) Photo of a 13 cm-long Japanese stalagmite, Kiro-1. (b) Enlarged section, 54–81 mm, with 19 subsamples from 16 layers for ^{230}Th dating. (c) Age model, established with the ^{230}Th dates with precisions of ±0.5% (vertical error bars). Horizontal bars represent the widths of drilled subsamples.

et al., 1999, 2008), long-term variability in the occurrence of tropical cyclones (e.g., Nott and Hayne, 2001), and giant tsunamis (e.g., Frohlich et al., 2009; Gong et al., 2012).

For century-old speleothem samples with ppm-level U, a ^{230}Th age precision of ±1 yr is achievable (Zhang et al., 2008). The small sample size requirement is particularly important for high-resolution dating of slow growth-rate samples. For speleothems containing 0.1 ppm ^{238}U age errors of 1–2% are routinely achievable for subsamples that are <100 mg in size. Comparable precision by ICP-SF-MS and TIMS typically required 5–50 times the sample size. High-resolution ^{230}Th dating will also be possible for sclerosponge (e.g., Swart et al., 2002).

Disadvantages include the non-linearity of SEM behavior with the RPQ turned on, which was not observed in TIMS and ICP-SF-MS. Fortunately, the additional intensity biases can be corrected using empirical formulas (Section 2.4.2). The intensity of ^{238}U ion beam could not be measured with our proposed SEM-only protocols. Protocols involving combined use of Faraday cups and SEM (e.g., Ball et al., 2008; Sims et al., 2008) can be used to overcome this obstacle; however, SEM yield correction should carefully be addressed. Due to high sensitivity, spectral interferences in MC-ICP-MS are 3–10 times higher than those in ICP-SF-MS. Additional oxidation steps should be taken to effectively remove organic material (Section 2.3) or the accuracy of the measurements may be compromised.

4. CONCLUSIONS

To precisely ^{230}Th-date small coral and speleothem carbonates a technique for determination of U–Th isotopic compositions and concentrations on MC-ICP-MS with SEM protocols has been developed. A series of long-term measurements of reference materials show that the analytical precision approximates counting statistics. This high-sensitivity technique allows small sample sizes, as low as 1–100 mg carbonate samples with sub-ppm-to-ppm U, and capacity for precise measurement of low Th samples, such as young corals and speleothems. The given examples of high-precision and high-resolution age models for a modern *Porites* coral with a hiatus and a stalagmite with slow growth rates indicate that our MC-ICP-MS techniques can offer precise and accurate calendar ages to combine with geochemical proxy records in coral, speleothem, and other carbonates for paleoclimatic and paleoenvironmental applications.

ACKNOWLEDGMENTS

We thank J. Schwieters, X. Wang, and B. Claudia for providing advice about instrumental techniques. We also thank H.-W. Chiang and N.D. Ngai for help with field work in Vietnam. Discussion with G.S. Burr of the University of Arizona was helpful. Constructive and comprehensive reviews by three anonymous reviewers significantly improved this paper. Funding for this research is provided by National Science Council Grants (98-2116-M-002-012, 99-2628-M-002-012, 100-2116-M-002-009, and 101-2116-M-002-009 to C.C.S.) and NSF Grants (1103403, 1103320, 0908792, and 0902867 to R.L.E.).

APPENDIX A

See Tables A1–A4.

Table A1
Duplicate U–Th isotopic measurements for old speleothem carbonates, WM1-H1, MO-1, and Kr-3.

Sample ID	^{238}U ppb	^{232}Th ppt	$^{230}Th/^{232}Th$ Atomic ratio, $\times 10^{-6}$	$^{234}U/^{238}U$ Atomic ratio, $\times 10^{-6}$	$^{234}U/^{238}U$ Activity ratio[a]	$^{230}Th/^{238}U$ Atomic ratio, $\times 10^{-6}$	$^{230}Th/^{238}U$ Activity ratio
WM1-H1a	20,923 ± 13	433.8 ± 2.3	795,699 ± 4244	54.953 ± 0.049	0.99969 ± 0.00089	16.927 ± 0.016	1.00068 ± 0.00094
WM1-H1b	18,400 ± 11	802.7 ± 3.0	377,804 ± 1435	54.987 ± 0.049	1.00031 ± 0.00089	16.909 ± 0.018	0.9996 ± 0.0011
WM1-H1c	17,587 ± 10	261.5 ± 2.2	11,08,620 ± 9469	54.928 ± 0.047	0.99924 ± 0.00086	16.912 ± 0.015	0.99980 ± 0.00089
WM1-H1d	30,445 ± 18	1189.7 ± 1.8	421,775 ± 676	54.923 ± 0.058	0.9991 ± 0.0011	16.909 ± 0.014	0.99962 ± 0.00083
WM1-H1e	27,026 ± 18	229.3 ± 1.2	19,42,534 ± 10,250	54.935 ± 0.071	0.9994 ± 0.0013	16.907 ± 0.015	0.99951 ± 0.00086
WM1-H1f	23,401 ± 13	1127.9 ± 1.9	342,124 ± 596	54.940 ± 0.055	0.9995 ± 0.0010	16.918 ± 0.014	1.00012 ± 0.00080
MO-1	936.93 ± 0.46	4.81 ± 0.29	32,10,483 ± 192,394	54.963 ± 0.055	0.9999 ± 0.0010	16.915 ± 0.018	0.9999 ± 0.0011
Kr-3	2249.4 ± 1.1	88.31 ± 0.29	420,170 ± 1417	54.999 ± 0.050	1.00053 ± 0.00090	16.923 ± 0.016	1.00045 ± 0.00095

Table A2
U–Th isotopic compositions and ^{230}Th ages for NTU coral standards, Coral-M and Coral-F, measured by ICP-SF-MS (Shen et al., 2002) and MC-ICP-MS (this study).

Standard ID	ICP-MS Method	^{238}U ppb	^{232}Th ppt	$\delta^{234}U$ Measured[a]	$[^{230}Th/^{238}U]$ Activity[c]	$[^{230}Th/^{232}Th]$ ppm[d]	Age Uncorrected	Age Corrected[c,e]	$\delta^{234}U_{initial}$ Corrected[b]
Coral-M	ICP-SF-MS	2534.0 ± 3.6	429.44 ± 0.60	147.5 ± 1.5	0.0001446 ± 0.0000054	14.07 ± 0.53	13.74 ± 0.52	8.99 ± 0.58	147.5 ± 1.5
	MC-ICP-MS	2537.0 ± 3.4	431.25 ± 0.45	145.4 ± 1.6	0.0001430 ± 0.0000024	13.87 ± 0.23	13.61 ± 0.23	8.84 ± 0.35	145.4 ± 1.6
Coral-F	ICP-SF-MS	2577.4 ± 1.9	4676.9 ± 8.7	143.6 ± 1.0	0.070623 ± 0.000241	641.7 ± 2.5	6942 ± 25	6892 ± 25	146.4 ± 1.1
	MC-ICP-MS	2574.8 ± 1.4	4679.5 ± 5.0	144.5 ± 1.1	0.070600 ± 0.000173	640.5 ± 1.7	6934 ± 19	6883 ± 19	147.3 ± 1.1

Analytical errors are 2σ of the mean.
[a] $\delta^{234}U = ([^{234}U/^{238}U]_{activity} - 1) \times 1000$.
[b] $\delta^{234}U_{initial}$ corrected was calculated based on ^{230}Th age (T), i.e., $\delta^{234}U_{initial} = \delta^{234}U_{measured} \times e^{\lambda_{234} \times T}$, and T is corrected age.
[c] $[^{230}Th/^{238}U]_{activity} = 1 - e^{-\lambda_{230}T} + (\delta^{234}U_{measured}/1000)[\lambda_{230}/(\lambda_{230} - \lambda_{234})](1 - e^{-(\lambda_{230} - \lambda_{234})T})$, where T is the age.
[d] The degree of detrital ^{230}Th contamination is indicated by the $[^{230}Th/^{232}Th]$ atomic ratio instead of the activity ratio.
[e] Age corrections were calculated using an $^{230}Th/^{232}Th$ atomic ratio of 4.86 (±0.27) ppm (Shen et al., 2008).

Table A3
U–Th isotopic compositions and ^{230}Th ages for speleothem subsamples measured by ICP-SF-MS (Shen et al., 2002) and MC-ICP-MS (this study).

Sample ID	ICP-MS Method	Weight g	^{238}U ppb	^{232}Th ppt	δ^{234}U Measured[a]	[^{230}Th/^{238}U] Activity[c]	[^{230}Th/^{232}Th] ppm[d]	Age Uncorrected	Age Corrected[c,e]	$\delta^{234}U_{initial}$ Corrected[b]
YK2-1a	ICP-SF-MS	0.1467	16,224 ± 68	4124 ± 11	29.2 ± 2.4	0.07817 ± 0.00043	5070 ± 22	8610 ± 53	8604 ± 53	29.9 ± 2.4
YK2-1b	MC-ICP-MS	0.0424	14,985 ± 26	5994 ± 28	42.5 ± 2.2	0.07936 ± 0.00022	3271 ± 17	8629 ± 31	8619 ± 31	43.5 ± 2.2
YK2-2a	ICP-SF-MS	0.1545	10,041 ± 31	4604 ± 17	27.8 ± 2.6	0.2011 ± 0.0011	7229 ± 43	23,717 ± 161	23,705 ± 161	29.7 ± 2.7
YK2-2b	MC-ICP-MS	0.0275	9599 ± 15	5719 ± 107	34.3 ± 1.8	0.20133 ± 0.00062	5571 ± 105	23,577 ± 94	23,562 ± 94	36.7 ± 2.0
YK2-4a	ICP-SF-MS	0.2593	3988 ± 17	2970.1 ± 8.3	114.5 ± 2.7	0.4635 ± 0.0024	10,263 ± 42	58,018 ± 438	58,001 ± 438	134.8 ± 3.2
YK2-4b	MC-ICP-MS	0.0607	4140.8 ± 7.6	2704 ± 19	118.6 ± 2.5	0.4638 ± 0.0013	11,712 ± 87	57,760 ± 277	57,744 ± 277	139.6 ± 2.9
YZ2-07-2a	ICP-SF-MS	0.3044	407.42 ± 0.80	8951 ± 21	2785.2 ± 5.9	2.6778 ± 0.0095	2009.6 ± 7.5	111,283 ± 654	111,162 ± 656	3811 ± 11
YZ2-07-2b	MC-ICP-MS	0.0310	407.61 ± 0.87	8993 ± 25	2775.9 ± 6.5	2.687 ± 0.011	2008.4 ± 9.2	112,321 ± 783	112,200 ± 784	3810 ± 12
YZ2-07-2c		0.0305	407.19 ± 0.87	9006 ± 27	2784.0 ± 7.8	2.685 ± 0.010	2001.6 ± 8.7	111,790 ± 747	111,669 ± 748	3815 ± 13
YZ2-07-2d		0.0320	407.31 ± 0.94	8994 ± 29	2782.6 ± 6.5	2.684 ± 0.011	2003.7 ± 9.5	111,767 ± 771	111,646 ± 772	3813 ± 12
YZ2-07-2e		0.0303	407.70 ± 0.91	9009 ± 26	2776.9 ± 8.8	2.687 ± 0.013	2005 ± 10	112,256 ± 929	112,134 ± 930	3810 ± 16
								Wt-averaged date	111,690 ± 400	

Analytical errors are 2σ of the mean.
Those are the values for a material at secular equilibrium, with the crustal ^{232}Th/^{238}U value of 3.8. The errors are arbitrarily assumed to be 50%.
[a] $\delta^{234}U = ([^{234}U/^{238}U]_{activity} - 1) \times 1000$.
[b] $\delta^{234}U_{initial}$ corrected was calculated based on ^{230}Th age (T), i.e., $\delta^{234}U_{initial} = \delta^{234}U_{measured} \times e^{\lambda_{234} \times T}$, and T is corrected age.
[c] $[^{230}Th/^{238}U]_{activity} = 1 - e^{-\lambda_{230}T} + (\delta^{234}U_{measured}/1000)[\lambda_{230}/(\lambda_{230} - \lambda_{234})](1 - e^{-(\lambda_{230} - \lambda_{234})T})$, where T is the age.
[d] The degree of detrital ^{230}Th contamination is indicated by the [^{230}Th/^{232}Th] atomic ratio instead of the activity ratio.
[e] Age corrections were calculated using an ^{230}Th/^{232}Th atomic ratio of 4 (±2) ppm.

Table A4
U–Th isotopic compositions and ^{230}Th ages for subsamples of coral ST0506 measured by ICP-SF-MS (Shen et al., 2002) and MC-ICP-MS (this study).

Subsample	ICP-MS	Weight	^{238}U	^{232}Th	$\delta^{234}U$	$[^{230}Th/^{238}U]$	$[^{230}Th/^{232}Th]$	Age	$\delta^{234}U_{initial}$	Age	^{230}Th Date
ID	Method	g	ppb	ppt	Measured[a]	Activity[c]	ppm[d]	Uncorrected	Corrected[b]	Corrected[c,e]	AD[f]
1a	ICP-SF-MS	0.6246	2504 ± 12	1103.3 ± 1.5	145.7 ± 1.2	0.0002974 ± 0.0000051	11.13 ± 0.18	28.31 ± 0.48	145.7 ± 1.2	20.17 ± 0.94	
1b		0.4872	2427 ± 11	810.8 ± 1.4	145.5 ± 1.8	0.0002757 ± 0.0000037	13.61 ± 0.18	26.25 ± 0.36	145.6 ± 1.8	20.07 ± 0.71	
1c		0.6181	2528 ± 11	1023.2 ± 1.5	145.7 ± 1.5	0.0002918 ± 0.0000043	11.89 ± 0.17	27.78 ± 0.41	145.7 ± 1.5	20.30 ± 0.85	
1d		0.4945	2485 ± 10	1222.3 ± 2.0	145.1 ± 1.4	0.0002830 ± 0.0000050	9.49 ± 0.16	26.95 ± 0.47	145.1 ± 1.4	17.9 ± 1.0	
									Wt-averaged date	19.76 ± 0.43	1987.59 ± 0.43
2a	ICP-SF-MS	0.8176	2592 ± 11	1553.7 ± 2.7	145.4 ± 1.7	0.0002944 ± 0.0000048	8.10 ± 0.13	28.03 ± 0.46	145.4 ± 1.7	17.0 ± 1.2	
2b		0.9258	2700 ± 11	1205.4 ± 2.6	145.5 ± 1.5	0.0002673 ± 0.0000041	9.87 ± 0.15	25.45 ± 0.39	145.5 ± 1.5	17.20 ± 0.91	
2c		0.6636	2648 ± 11	1481.3 ± 2.3	146.2 ± 1.5	0.0002771 ± 0.0000046	8.17 ± 0.13	26.36 ± 0.44	146.2 ± 1.5	16.0 ± 1.1	
2d		0.8849	2554 ± 11	1493.2 ± 2.5	145.5 ± 1.5	0.0002953 ± 0.0000049	8.33 ± 0.14	28.11 ± 0.47	145.5 ± 1.5	17.3 ± 1.2	
									Wt-averaged date	16.90 ± 0.54	1990.45 ± 0.54
3a	MC-ICP-MS	0.2511	2059 ± 11	673.5 ± 1.7	146.2 ± 1.1	0.0001612 ± 0.0000079	8.13 ± 0.40	15.34 ± 0.75	146.2 ± 1.1	9.3 ± 1.0	
3b		0.3303	1847 ± 10	700.5 ± 1.2	146.0 ± 1.2	0.0001755 ± 0.0000051	7.63 ± 0.22	16.71 ± 0.48	146.0 ± 1.2	9.70 ± 0.85	
3c		0.3584	1900 ± 10	718.3 ± 1.2	143.3 ± 1.2	0.0001660 ± 0.0000049	7.24 ± 0.21	15.83 ± 0.47	143.3 ± 1.2	8.83 ± 0.84	
3d		0.2305	3250 ± 22	1328.6 ± 3.5	145.1 ± 1.3	0.0001917 ± 0.0000060	7.73 ± 0.24	18.26 ± 0.57	145.1 ± 1.3	10.70 ± 0.94	
									Wt-averaged date	9.60 ± 0.45	1998.21 ± 0.45
4a	MC-ICP-MS	0.1655	2133 ± 12	632.6 ± 3.1	142.3 ± 1.6	0.0001818 ± 0.0000076	10.11 ± 0.42	17.36 ± 0.73	142.3 ± 1.6	11.87 ± 0.91	
4b		0.2336	1983 ± 11	724 ± 11	143.0 ± 1.6	0.0001878 ± 0.0000068	8.47 ± 0.31	17.91 ± 0.65	143.0 ± 1.6	11.15 ± 0.93	
4c		0.3305	1802.3 ± 9.2	1351.5 ± 4.3	144.8 ± 1.4	0.0002625 ± 0.0000088	5.77 ± 0.19	25.01 ± 0.84	144.8 ± 1.4	11.1 ± 1.6	
4d		0.3233	1795.3 ± 8.9	794.3 ± 2.2	147.3 ± 1.4	0.0002142 ± 0.0000063	7.98 ± 0.23	20.36 ± 0.60	147.3 ± 1.4	12.2 ± 1.0	
									Wt-averaged date	11.66 ± 0.52	1996.15 ± 0.52

Analytical errors are 2σ of the mean.
[a] $\delta^{234}U = ([^{234}U/^{238}U]_{activity} - 1) \times 1000$.
[b] $\delta^{234}U_{initial}$ corrected was calculated based on ^{230}Th age (T), i.e., $\delta^{234}U_{initial} = \delta^{234}U_{measured} \times e^{\lambda_{234} \times T}$, and T is corrected age.
[c] $[^{230}Th/^{238}U]_{activity} = 1 - e^{-\lambda_{230}T} + (\delta^{234}U_{measured}/1000)[\lambda_{230}/(\lambda_{230} - \lambda_{234})](1 - e^{-(\lambda_{230} - \lambda_{234})T})$, where T is the age.
[d] The degree of detrital ^{230}Th contamination is indicated by the $[^{230}Th/^{232}Th]$ atomic ratio instead of the activity ratio.
[e] Age corrections were calculated using an $^{230}Th/^{232}Th$ atomic ratio of 3.2 (±0.32) ppm (Shen et al., 2008).
[f] Chemistry date: 2007/04/06 for subsamples from 1a to 2d, 2007/09/22 from 3a to 4d.

REFERENCES

Andersen M. B., Stirling C. H., Potter E. K. and Halliday A. N. (2004) Toward epsilon levels of measurement precision on $^{234}U/^{238}U$ by using MC-ICPMS. *Int. J. Mass Spectrom.* **237**, 107–118.

Andersen M. B., Stirling C. H., Porcelli D., Halliday A. N., Andersson P. S. and Baskaran M. (2007) The tracing of riverine U in Arctic seawater with very precise $^{234}U/^{238}U$ measurements. *Earth Planet. Sci. Lett.* **259**, 171–185.

Andersen M. B., Stirling C. H., Potter E.-K., Halliday A. N., Blake S. G., McCulloch M. T., Ayling B. F. and O'Leary M. (2008) High-precision U-series measurements of more than 500,000 year old fossil corals. *Earth Planet. Sci. Lett.* **265**, 229–245.

Ball L., Sims K. W. W. and Schwieters J. (2008) Measurement of $^{234}U/^{238}U$ and $^{230}Th/^{232}Th$ in volcanic rocks using the Neptune MC-ICP-MS. *J. Anal. Atomic Spectrom.* **23**, 173–180.

Barnes J. W., Lang E. J. and Potratz H. A. (1956) Ratio of ionium to uranium in coral limestone. *Science* **124**, 175–176.

Bourdon B., Henderson G. M., Lundstrom C. C. and Turner S. P. (2003) *Uranium-Series Geochemistry*. Mineralogical Society of America, Washington, DC.

Brennecka G. A., Borg L. E., Hutcheon I. D., Sharp M. A. and Anbar A. D. (2010) Natural variations in uranium isotope ratios of uranium ore concentrates: Understanding the $^{238}U/^{235}U$ fractionation mechanism. *Earth Planet. Sci. Lett.* **291**, 228–233.

Broecker W. S. and Thurber D. L. (1965) Uranium-series dating of corals and oolites from Bahaman and Florida Key limestones. *Science* **149**, 58–60.

Chen J. H., Edwards R. L. and Wasserburg G. J. (1986) ^{238}U, ^{234}U and ^{232}Th in seawater. *Earth Planet. Sci. Lett.* **80**, 241–251.

Cheng H., Edwards R. L., Hoff J., Gallup C. D., Richards D. A. and Asmerom Y. (2000) The half-lives of uranium-234 and thorium-230. *Chem. Geol.* **169**, 17–33.

Cheng H., Edwards R. L., Broecker W. S., Denton G. H., Kong X., Wang Y., Zhang R. and Wang X. (2009) Ice age terminations. *Science* **326**, 248–252.

Cheng H., Zhang P. Z., Spötl C., Edwards R. L., Cai Y. J., Zhang D. Z., Sang W. C., Tan M. and An Z. S. (2012a) The climatic cyclicity in semiarid- arid central Asia over the past 500,000 years. *Geophys. Res. Lett.* **39**, L01705. http://dx.doi.org/10.1029/2011GL050202.

Cheng H., Edwards R. L., Shen C.-C., Polyak V. J., Asmerom Y., Woodhead J., Hellstrom J., Wang Y., Kong X. and Spötl C. (2012b) Improvements in ^{230}Th dating, ^{230}Th and ^{234}U half-life values, and U–Th isotopic measurements by multi-collector inductively coupled plasma mass spectroscopy. *Earth Planet. Sci. Lett.* (in revision).

Cobb K. M., Charles C. D., Cheng H. and Edwards R. L. (2003) El Niño/Southern Oscillation and tropical Pacific climate during the last millennium. *Nature* **424**, 271–276.

DeLong K., Quinn T. M., Taylor F. W., Lin K. and Shen C.-C. (2012) Sea surface temperature variability in the southwest tropical Pacific since AD 1649. *Nat. Clim. Change* **2**. http://dx.doi.org/10.1038/nclimate1583.

Dorale J. A., Edwards R. L., Ito E. and González L. A. (1998) Climate and vegetation history of the midcontinent from 75 to 25 ka: A speleothem record from Crevice Cave, Missouri, USA. *Science* **282**, 1871–1874.

Dorale J. A., Edwards R. L., Alexander, Jr., E. C., Shen C.-C., Richards D. A. and Cheng H. (2004) Uranium-series dating of speleothems: Current techniques, limits, and applications. In *Studies of Cave Sediments: Physical and Chemical Records of Paleoclimate* (eds. J. Mylroie and I. D. Sasowsky). Kluwer Academic/Plenum Publishers, New York, pp. 177–197.

Douville E., Sallé E., Frank N., Eisele M., Pons-Branchu E. and Ayrault S. (2011) Rapid and accurate U–Th dating of ancient carbonates using inductively coupled plasma-quadrupole mass spectrometry. *Chem. Geol.* **272**, 1–11.

Edwards R. L., Chen J. H. and Wasserburg G. J. (1986/87) ^{238}U–^{234}U–^{230}Th–^{232}Th systematics and the precise measurement of time over the past 500,000 years. *Earth Planet. Sci. Lett.* **81**, 175–192.

Edwards R. L. (1988) High precision thorium-230 ages of corals and the timing of sea level fluctuation in the late Quaternary. Ph. D. thesis, California Institute of Technology.

Edwards R. L., Taylor F. W. and Wasserburg G. J. (1988) Dating earthquakes with high-precision Th-230 ages of very young corals. *Earth Planet. Sci. Lett.* **90**, 371–381.

Edwards R. L., Gallup C. D. and Cheng H. (2003) Uranium-series dating of marine and lacustrine carbonates. In *Uranium-Series Geochemistry* (eds. B. Bourdon, G. M. Henderson, C. C. Lundstrom and S. P. Turner). Mineralogical Society of America, Washington, DC, pp. 363–405.

Fairchild I. J., Smith C. L., Baker A., Fuller L., Spötl C., Mattey D. and McDermott F.E.I.M.F. (2006) Modification and preservation of environmental signals in speleothems. *Earth Sci. Rev.* **75**, 105–153.

Fairchild I. J. and Treble P. C. (2009) Trace elements in speleothems as recorders of environmental change. *Quat. Sci. Rev.* **28**, 449–468.

Fleitmann D., Burns S. J., Mangini A., Mudelsee M., Kramers J., Villa I., Neff U., Al-Subbary A. A., Buettner A., Hippler D. and Matter A. (2007) Holocene ITCZ and Indian monsoon dynamics recorded in stalagmites from Oman and Yemen (Socotra). *Quat. Sci. Rev.* **26**, 170–188.

Frohlich C., Hornbach M. J., Taylor F. W., Shen C.-C., Moala A., Morton A. E. and Kruger J. (2009) Huge erratic boulders in Tonga deposited by a prehistoric tsunami. *Geology* **37**, 131–134.

Gagan M. K., Ayliffe L. K., Beck J. W., Cole J. E., Druffel E. R. M., Dunbar R. B. and Schrag D. P. (2000) New views of tropical paleoclimates from corals. *Quat. Sci. Rev.* **19**, 45–64.

Goldstein S. J. and Stirling C. H. (2003) Techniques for measuring uranium-series nuclides: 1992–2002. *Rev. Mineral. Geochem.* **52**, 23–57.

Gong S.-Y., Wu T.-R., Siringan F. P., Lin K. and Shen C.-C. (2012) An abrupt backreef infilling in a Holocene reef, Paraoir, Northwestern Luzon, Philippines. *Coral Reefs* (in revision).

Griffiths M. L., Drysdale R. N., Gagan M. K., Zhao J.-x., Ayliffe L. K., Hellstrom J. C., Hantoro W. S., Frisia S., Feng Y.-x., Cartwright I., Pierre E. St., Fischer M. J. and Suwargadi B. W. (2009) Increasing Australian–Indonesian monsoon rainfall linked to early Holocene sea-level rise. *Nat. Geosci.* **2**, 636–639.

Grottoli A. G. and Eakin C. M. (2007) A review of modern coral $\delta^{18}O$ and $\delta^{14}C$ proxy records. *Earth Sci. Rev.* **81**, 67–91.

Halliday A. N., Lee D.-C., Christensen J. N., Rehkamper M., Yi W., Luo X.-Z., Hall C. M., Ballentine C. J., Pettke T. and Stirling C. (1998) Applications of multiple collector-ICPMS to cosmochemistry, geochemistry, and paleoceanography. *Geochim. Cosmochim. Acta* **62**, 919–940.

Hayes J. M. and Schoeller D. A. (1977) High precision pulse counting: Limits and optimal conditions. *Anal. Chem.* **49**, 306–311.

Hiess J., Condon D. J., McLean N. and Noble S. R. (2012) $^{238}U/^{235}U$ systematics in terrestrial uranium-bearing minerals. *Science* **355**, 1610–1614.

Hoffmann D. L., Richards D. A., Elliott T. R., Smart P. L., Coath C. D. and Hawkesworth C. J. (2005) Characterisation of

secondary electron multiplier nonlinearity using MC-ICPMS. *Int. J. Mass Spectrom.* **244**, 97–108.

Hoffmann D. L., Prytulak J., Richards D. A., Elliott T., Coath C. D., Smart P. L. and Scholz D. (2007) Procedures for accurate U and Th isotope measurements by high precision MC-ICPMS. *Int. J. Mass Spectrom.* **264**, 97–109.

Ivanovich M. and Harmon R. S. (1992) *Uranium-Series Disequilibrium*, second ed. Clarendon Press, Oxford.

Jaffey A. H., Flynn K. F., Glendenin L. E., Bentley W. C. and Essling A. M. (1971) Precision measurement of half-lives and specific activities of ^{235}U and ^{238}U. *Phys. Rev. C* **4**, 1889–1906.

Jiang X., He Y., Shen C.-C., Kong X., Guo Y., Li Z. and Chang Y.-W. (2012) Stalagmite-inferred Holocene precipitation in northern Guizhou Province and asynchronous ending of the Climatic Optimum in the Asian monsoon territory. *Chinese Sci. Bull.* **57**, 73–79.

Kanner L. C., Burns S. J., Cheng H. and Edwards R. L. (2012) High-latitude forcing of the South American summer monsoon during the last glacial. *Science* **335**, 570–573.

Lachniet M. S. (2009) Climatic and environmental controls on speleothem oxygen-isotope values. *Quat. Sci. Rev.* **28**, 412–432.

Li T.-Y., Shen C.-C., Li H.-C., Li J.-Y., Chiang H.-W., Song S.-R., Yuan D.-X., Wang J.-L., Ye M.-Y., Tang L.-L. and Xie S.-Y. (2011) Oxygen and carbon isotopic systematics of aragonite speleothems and water in Furong Cave, Chongqing, China. *Geochim. Cosmochim. Acta* **75**, 4140–4156.

Luo X., Rehkämper M., Lee D.-C. and Halliday A. N. (1997) High precision ^{230}Th/^{232}Th and ^{234}U/^{238}U measurements using energy-filtered ICP magnetic sector multiple collector mass spectrometry. *Int. J. Mass Spectrom.* **171**, 105–117.

Ludwig K. A., Shen C.-C., Kelly D. S., Cheng H. and Edwards R. L. (2011) U–Th systematics and ^{230}Th ages of carbonate chimneys at the Lost City Hydrothermal Field. *Geochim. Cosmochim. Acta* **75**, 1869–1888.

Meyer M. C., Cliff R. A., Spötl C., Knipping M. and Mangini A. (2009) Speleothems from the earliest Quaternary: Snapshots of paleoclimate and landscape evolution at the northern rim of the Alps. *Quat. Sci. Rev.* **28**, 1374–1391.

Nott J. and Hayne M. (2001) High frequency of 'super-cyclones' along the Great Barrier Reef over the past 5000 years. *Nature* **413**, 508–511.

Pietruszka A. J., Carlson R. W. and Hauri E. H. (2002) Precise and accurate measurement of ^{226}Pa–^{230}Th–^{238}U disequilibria in volcanic rocks using plasma ionization multicollector mass spectrometry. *Chem. Geol.* **188**, 171–191.

Richards D. A. and Dorale J. A. (2003) Uranium-series chronology and environmental applications of speleothems. In *Uranium-Series Geochemistry* (eds. B. Bourdon, G. M. Henderson, C. C. Lundstrom and S. P. Turner). Mineralogical Society of America, Washington, DC, pp. 407–460.

Richter S., Goldberg S. A., Mason P. B., Traina A. J. and Schwieters J. B. (2001) Linearity tests for secondary electron multipliers used in isotope ratio mass spectrometry. *Int. J. Mass Spectrom.* **206**, 105–127.

Richter S., Alonso A., Aregbe Y., Eykens R., Kehoe F., Kühn H., Kivel N., Verbruggen A., Wellum R. and Taylor P. D. P. (2009) A new series of uranium isotope reference materials for investigating the linearity of secondary electron multipliers in isotope mass spectrometry. *Int. J. Mass Spectrom.* **281**, 115–125.

Richter S., Eykens R., Kühn H., Aregbe Y., Verbruggen A. and Weyer S. (2010) New average values for the n(^{238}U)/n(^{235}U) isotope ratios of natural uranium standards. *Int. J. Mass Spectrom.* **295**, 94–97.

Shaw T. J. and Francois R. (1991) A fast and sensitive ICP-MS assay for the determination of ^{230}Th in marine sediments. *Geochim. Cosmochim. Acta* **55**, 2075–2078.

Shen G. T. (1996) Rapid change in the tropical ocean and the use of corals as monitoring systems. In *Geoindicators: Assessing Rapid Environmental Changes in Earth Systems* (eds. A. R. Berger and W. J. Iams). A.A. Balkema Publishers, VT, USA, pp. 155–169.

Shen C.-C., Edwards R. L., Cheng H., Dorale J. A., Thomas R. B., Moran S. B., Weinstein S. E. and Edmonds H. N. (2002) Uranium and thorium isotopic and concentration measurements by magnetic sector inductively coupled plasma mass spectrometry. *Chem. Geol.* **185**, 165–178.

Shen C.-C., Cheng H., Edwards R. L., Moran S. B., Edmonds H. N., Hoff J. A. and Thomas R. B. (2003) Measurement of attogram quantities of ^{231}Pa in dissolved and particulate fractions of seawater by isotope dilution thermal ionization mass spectroscopy. *Anal. Chem.* **75**, 1075–1079.

Shen C.-C., Lee T., Liu K.-K., Hsu H.-H., Edwards R. L., Wang C.-H., Lee M.-Y., Chen Y.-G., Lee H.-J. and Sun H.-T. (2005) An evaluation of quantitative reconstruction of past precipitation records using coral skeletal Sr/Ca and δ^{18}O data. *Earth Planet. Sci. Lett.* **237**, 370–386.

Shen C.-C., Lin H.-T., Chu M.-F., Yu E.-F., Wang X. and Dorale J. A. (2006) Measurement of natural uranium concentration and isotopic composition with permil-level precision by inductively coupled plasma quadrupole mass spectrometry. *Geochem. Geophys. Geosyst.* **7**, Q09005. http://dx.doi.org/10.1029/2006GC001303.

Shen C.-C., Chiu H.-Y., Chiang H.-W., Chu M.-F., Wei K.-Y., Steinke S., Chen M.-T., Lin Y.-S. and Lo L. (2007) High precision measurements of Mg/Ca and Sr/Ca ratios in carbonates by cool plasma inductively coupled plasma quadrupole mass spectrometry. *Chem. Geol.* **236**, 339–349.

Shen C.-C., Li K.-S., Sieh K., Natawidjaja D. H., Cheng H., Wang X., Edwards R. L., Lam D. D., Hsieh Y.-T., Fan T.-Y., Meltzner A. J., Taylor F. W., Quinn T. M., Chiang H.-W. and Kilbourne K. H. (2008) Variation of initial ^{230}Th/^{232}Th and limits of high precision U–Th dating of shallow-water corals. *Geochim. Cosmochim. Acta* **72**, 4201–4223.

Shen C.-C., Kano A., Hori M., Lin K., Chiu T.-C. and Burr G. S. (2010) East Asian monsoon evolution and reconciliation of climate records from Japan and Greenland during the last deglaciation. *Quat. Sci. Rev.* **29**, 3327–3335.

Sieh K., Ward S. N., Natawidjaja D. H. and Suwargadi B. W. (1999) Crustal deformation at the Sumatran subduction zone revealed by coral rings. *Geophys. Res. Lett.* **26**, 3141–3144.

Sieh K., Natawidjaja D. H., Meltzner A. J., Shen C.-C., Suwargadi B. W., Galetzka J., Cheng H., Li K.-S. and Edwards R. L. (2008) Earthquake supercycles inferred from sea-level changes recorded in the corals of West Sumatra. *Science* **322**, 1674–1678.

Siklósy Z., Demény A., Vennemann T. W., Pilet S., Kramers J., Leél-Össsy S., Bondár M., Shen C.-C. and Hegner E. (2009) Bronze Age volcanic event recorded in stalagmites by combined isotope and trace element studies. *Rapid Commun. Mass Spectrom.* **23**, 801–808.

Sims K. W. W., Gill J. B., Dosseto A., Hoffmann D. L., Lundstrom C. C., Williams R. W., Ball L., Tollstrup D., Turner S., Prytulak J., Glessner J. J. G., Standish J. J. and Elliott T. (2008) An inter-laboratory assessment of the thorium isotopic composition of synthetic and rock reference materials. *Geostand. Geoanal. Res.* **32**, 65–91.

Sinha A., Stott L., Berkelhammer M., Cheng H., Edwards R. L., Buckley B., Aldenderfer M. and Mudelsee M. (2011) A global context for megadroughts in monsoon Asia during the past millennium. *Quat. Sci. Rev.* **30**, 47–62.

Stirling C. H., Andersen M. B., Potter E.-K. and Halliday A. N. (2007) Low temperature isotope fractionation of uranium. *Earth Planet. Sci. Lett.* **264**, 208–225.

Stirling C. H. and Andersen M. B. (2009) Uranium-series dating of fossil coral reefs: Extending the sea-level record beyond the last glacial cycle. *Earth Planet. Sci. Lett.* **284**, 269–283.

Swart P. K., Thorrold S., Rosenheim B., Eisenhauer A., Harrison C. G. A., Grammer M. and Latkoczy C. (2002) Intra-annual variation in the stable oxygen and carbon and trace element composition of sclerosponges. *Paleoceanography* **17**, 1045. http://dx.doi.org/10.1029/2000PA000622.

Taylor F. W., Edwards R. L. and Wasserburg G. J. (1990) Seismic recurrence intervals and timing of aseismic subduction inferred from emerged corals and reefs of the central Vanuatu (New Hebrides) frontal arc. *J. Geophys. Res.* **95**, 393–408.

Wang Y., Cheng H., Edwards R. L., An Z., Wu J., Shen C.-C. and Dorale J. A. (2001) A high resolution absolute dated record of the East Asian Monsoon from 11,000 to 75,000 years B.P. from Hulu Cave, China. *Science* **294**, 2345–2348.

Wang X., Auler A. S., Edwards R. L., Cheng H., Cristalli P. S., Smart P. L., Richards D. A. and Shen C.-C. (2004) Northeastern Brazil wet periods linked to distant climate anomalies and rainforest boundary changes. *Nature* **432**, 740–743.

Wang Y., Cheng H., Edwards R. L., He Y., Kong X., An Z., Wu J., Kelly M., Dykoski C. A. and Li X. (2005) The Holocene Asian monsoon: Links to solar changes and North Atlantic climate. *Science* **308**, 854–857.

Wang Y., Cheng H., Edwards R. L., Kong X., Shao X., Chen S., Wu J., Jiang X., Wang X. and An Z. (2008) Millennial- and orbital-scale changes in the East Asian monsoon over the past 224,000 years. *Nature* **451**, 1090–1093.

Weyer S., Anbar A. D., Gerdes A., Gordon G. W., Algeo T. J. and Boyle E. A. (2008) Natural fractionation of $^{238}U/^{235}U$. *Geochim. Cosmochim. Acta* **72**, 345–359.

Wieser M. E. and Schwieters J. B. (2005) The development of multiple collector mass spectrometry for isotope ratio measurements. *Int. J. Mass Spectrom.* **242**, 97–115.

Woodhead J., Hellstroma J., Maasa R., Drysdaleb R., Zanchettac G., Devined P. and Taylord Y. (2006) U-Pb geochronology of speleothems by MC-ICPMS. *Quat. Geochronol.* **1**, 208–221.

Yuan D., Cheng H., Edwards R. L., Dykoski C. A., Kelly M. J., Zhang M., Qing J., Lin Y., Wang Y., Wu J., Dorale J. A., An Z. and Cai Y. (2004) Timing, duration, and transitions of the last interglacial Asian monsoon. *Science* **304**, 575–578.

Zhang P., Cheng H., Edwards R. L., Chen F., Wang Y., Yang X., Liu J., Tan M., Wang X., Liu J., An C., Dai Z., Zhou J., Zhang D., Jia J., Jin L. and Johnson K. R. (2008) A test of climate, sun, and culture relationships from an 1810-year Chinese cave record. *Science* **322**, 940–942.

Zhao J.-x., Yu K.-f. and Feng Y.-x. (2009) High-precision ^{238}U–^{234}U–^{230}Th disequilibrium dating of the recent past: A review. *Quat. Geochronol.* **4**, 423–433.

Associate editor: Peter Ulmer